Improvement of Artificial Auscultation on Hemodialysis Stenosis by the Estimate of Stenosis Site and the Hierarchical Categorization of Learning Data

Hatsuhiro KATO[†a)], *Member*, **Masakazu KIRYU**[†], *Nonmember*, **Yutaka SUZUKI**[††], **Osamu SAKATA**[†], *Members*, *and* **Mizuya FUKASAWA**[†††], *Nonmember*

SUMMARY   Many hemodialysis patients undergo plasitc surgery to form the arterio-venous fistula (AVF) in their forearm to improve the vascular access by shunting blood flows. The issue of AVF is the stenosis caused by the disturbance of blood flows; therefore the auscultation system to assist the stenosis diagnosis has been developed. Although the system is intended to be used as a steady monitoring for stenosis assessment, its efficiency was not always high because it cannot estimate where the stenosis locates. In this study, for extracting and estimating the stenosis signal, the shunt murmurs captured by many microphones were decomposed by the principal component analysis (PCA). Furthermore, applying the hierarchical categorization of the recursive subdivision self-organizing map (rs-SOM), the modelling of the stenosis signal was proposed to realise the effective stenosis assessment. The false-positive rate of the stenosis assessment was significantly reduced by using the improved auscultation system.
key words: auscultation, hemodialysis, shunt murmur, stenosis, PCA, rs-SOM

1.   Introduction

For improving the vascular access, many of hemodialysis patients undergo a plastic surgery to form the arterio-venous fistula (AVF) by shunting the blood flow in the artery to the vein in their forearm [1]. The issue with AVF lies in the possibility of stenosis occurring in the vessels due to shear stress [2]. Therefore, it is necessary not only to make a regular diagnoses regarding the states of vessels but to restore the blood flow on an as-needed basis by percutaneous transluminal angioplasty (PTA) [3]. The success rate of PTA tends to deteriorate when the stenosis level increases. Therefore, the steady monitoring and the early detection of stenosis are important.

It is well known that the unique beat sounds are monitored from vessels with AVF as a result of the structure [4], which is termed as shunt murmur and used to diagnose the stenosis by the auscultation. The auscultation skill depends on experience; furthermore, the criterion is not always apparent. Therefore, an assessment system to support the stenosis diagnosis has been developed with various ways using the frequency analysis [5], the wavelet analysis [6], [7], hidden Markov process [8] and non-steady analysis [9]. One of the promising systems among all of those is the artificial assessment system that uses the database composed by various shunt murmurs [10], [11]. However, the efficiency of the stenosis assessment was not always high because the system can not effectively estimate where the stenosis is located.

In this study, for extracting stenosis signals and estimating the stenosis site, shunt murmurs which were captured by many microphones along the vein at forearm were decomposed with the principal component analysis (PCA) [12] and categorized to construct model vectors with self-organizing map (SOM) [14]. The PCA is a method to develop the multi-components signal into the linear combination of the principal components according to the magnitude of their variances. The component with the smallest variance can be regarded as the component that is less affected by the common signal caused by the heartbeat and reflects the peculiar information due to the captured location. The murmur vector was composed of the principal components to express the peculiar information from the stenosis site.

Recursive subdivision self-organized map (rs-SOM) is the method to categorize hierarchically the learning data [11]. This method allocates the model vector to each subdivided category with interpolating the difference between the categories. In this study, using these model vectors, new stenosis level was defined and used to improve the efficiency of the stenosis assessment.

This paper is organized as follows. In Sect. 2, the components of assessment system is described focusing on capturing from multi-sites and the decomposing the stenosis signals by PCA. The murmur vector is defined with spectra of the principal components. The stenosis site can be estimated using a distance defined by murmur vectors. In Sect. 3, the empirical and SOM categories are defined using the learning data being composed by typical shunt murmurs. To define he SOM category, the hierarchical categorization realized by rs-SOM plays an important role. Futhermore, the new assessment criterion is proposed using the stenosis level, which leads to an improvement of the artificial auscul-

[†]The authors are with Faculty of Engineering, Graduate School, University of Yamanashi, Kofu-shi, 400–8511 Japan.
[†]The author is with Center for Life Science Research, Graduate School, University of Yamanashi, Chuo-shi, 409–3898 Japan.
[†††]The author is with Division of Medicine Clinical Medicine Science, Graduate School, University of Yamanashi, Chuo-shi, 409–3898 Japan.
a) E-mail: katoh@yamanashi.ac.jp

tation. The efficiency of the stenosis assessment is evaluated by the false-positive rate of the threshold criterion. The last section is devoted to conclusions.

2. Characterization of Murmurs by PCA

2.1 Stenosis Signal Captured from Multiple Sites

As shown in Fig. 1 (a), from patients who needed to expand the blood vessel with the surgery PTA, blood flow sounds were captured with $L(=4)$ microphones aligned on the vein from the wrist to the elbow in their forearm. The blood flow sounds were capture before and after PTA, which were specified by the index $\sigma(= \text{bfr/aft})$ and numbered from the wrist as $\ell(=1,2\ldots,L)$. The P pulses involved in heartbeats are extracted and denoted as the time function $x_{\ell,\sigma}^{(p)}(t)$ ($p = 1, 2, \ldots, P$) with the time t, the pulse index p and the location index ℓ. Using the sampling frequency F_s and the total data number per pulse N_{time}, the time t can be discretized as $t_n = n/Fs$ ($n = 0, 1, 2, \ldots, N_{\text{time}} - 1$). The pulse data should be loaded on block diagram shown in Fig. 1 (b). The pulses are characterized and transformed into murmur vector as defined in later section. The characterized data are subject to the assessment process using the categories accumulated in the data base [10], [11]. New procedures proposed in this study are mainly associated with the blocks of the 'murmur vector' and the 'data base'.

The L-dimensional column vector $\mathbf{x}_\sigma^{(p)}(t)$ can be composed of the sound pressures $x_{\ell,\sigma}^{(p)}(t)$ being allocated to the ℓ-th component. The correlation between the captured sites is expressed by the fact that the end point of vector $\mathbf{x}_\sigma^{(p)}(t)$ is on the hyperplane with the normal vector $\mathbf{e}$. Then, the displacement from the hyperplane can be regarded as the peculiar component due to the captured site. The magnitude of the displacement can be evaluated by the variance defined by $v_\sigma = \mathbf{e} \cdot \mathbf{\Sigma}_\sigma \mathbf{e}$. Here, $\mathbf{\Sigma}_\sigma$ is the covariance matrix [12] that is defined by

$$\mathbf{\Sigma}_\sigma = \frac{1}{PN_{\text{time}}} \sum_{p=1}^{P} \sum_{n=0}^{N_{\text{time}}-1} \mathbf{x}_\sigma^{(p)}(t_n)\left\{\mathbf{x}_\sigma^{(p)}(t_n)\right\}^T. \qquad (1)$$

The (ℓ, ℓ')-component of $\mathbf{\Sigma}_\sigma$ is the average of the product $x_{\ell,\sigma}^{(p)}(t_n)x_{\ell',\sigma}^{(p)}(t_n)$ about all of N_{time} times and P pulses.

The problem to find the normal vector $\mathbf{e}_\sigma$ that gives local minimum of v_σ is equivalent to the eigenvalue problem that satisfies the relation

$$\mathbf{\Sigma}_\sigma \mathbf{e}_\sigma = v_\sigma \mathbf{e}_\sigma. \qquad (2)$$

Because the matrix $\mathbf{\Sigma}_\sigma$ is symmetrix, the eigen values satisfy the orthogonal relation; $\mathbf{e}_{\ell,\sigma} \cdot \mathbf{e}_{\ell',\sigma} = \delta_{\ell,\ell'}$ where $\delta_{\ell,\ell'}$ is Kroneker's delta. When the eigenvalues and eigenvectors are numbered as $1, 2, \ldots, L (= \ell)$ in order of the magnitude of eigenvalues, the quantity $y_{\ell,\sigma}^{(p)}(t) = \mathbf{e}_{\ell,\sigma} \cdot \mathbf{x}_\sigma^{(p)}(t)$ is termed as the ℓ-th principal component [12]. Using the orthogonal relation of eigenvalues, the vector $\mathbf{x}_\sigma^{(p)}(t)$ can be developed in series as follows:
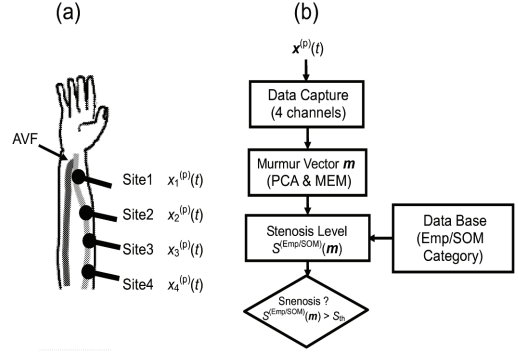

Fig. 1 System of stenosis assessment. (a) Data capturing from four sites. (b) Block diagram of the assessment process.
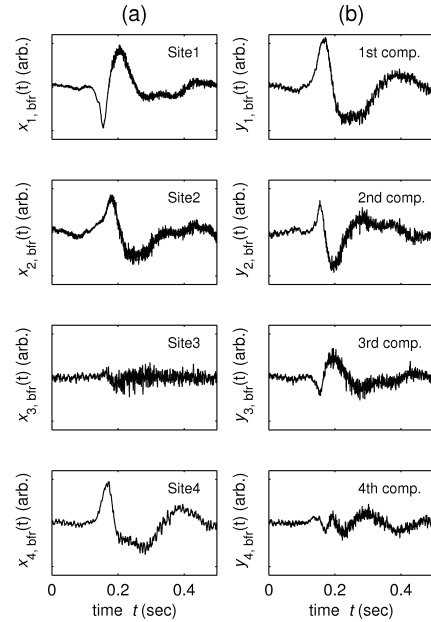

Fig. 2 Shunt murmurs in time domain. Variation due to (a) capture sites, $x_{\ell,\text{bfr}}(t)$, and (b) pricipal components, $y_{\ell,\text{bfr}}(t)$ ($\ell = 1, 2, 3, 4$).

$$\mathbf{x}_\sigma^{(p)}(t) = \sum_{\ell=1}^{L} y_{\ell,\sigma}^{(p)}(t)\mathbf{e}_{\ell,\sigma}. \qquad (3)$$

In Fig. 2, the change of the sound pressures which were captured before the surgery PTA. The panel column of (a) shows the averages over the pulses $x_{\ell,\text{bfr}}(t) = P^{-1}\sum_{p=1}^{P} x_{\ell,\text{bfr}}^{(p)}(t)$ at each site ℓ. The panel column of (b) shows the average of the principal components $y_{\ell,\text{bfr}}(t) = P^{-1}\sum_{p=1}^{P} y_{\ell,\text{bfr}}^{(p)}(t)$. For each capturing, the serial pulses were collected during 30 sec and the $21(= P)$ pulses of 0.5 sec length were extracted. The length, 0.5 sec, was determined to separate the serial pulses without any overlap. All pulses are normalized such that the peak centre is located at the first 2/5 of pulse length and the sum of squares has to be unity. We had examined the long pulses of 0.6 sec and 1.0 sec, but the result was not affected substantially by the pulse length. The number of microphones, $L = 4$, was determined so as to be easy to set up at the clinical field. Further investigation on
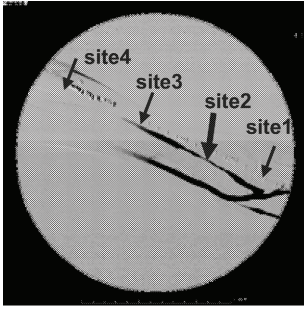
Fig. 3 Angiography of shunted vessels. The stenosis occurs at site 2.

the multi-channel sensor with many microphones was also discussed in the another work [13]. Although the acoustic apparatus has the sampling rate of 44,100 Hz, the sampling rate was converted into $F_s = 4,410$ Hz because the stenosis signal did not exceed the frequency 2,000 Hz. Therefore, the total sampling number per pulse is $N_{\text{time}} = 2,205$.

According to the data of time domain shown in Fig. 2 (a), the behaviour of site 3 is different from others. The small but finite trembling behaviour is also observed in later half of the time domain at site 3 and site 2. Therefore, the stenosis would be estimated to exist at the site 3 or 2. In fact, the stenosis was found at the site 2 by observing the vessels using the angiography as shown in Fig. 3. The unique behaviour of site 3 can be regarded as due to the turbulence of blood flow at site 2. A detailed consideration on the turbulence in vessels with stenosis is reviewed in Ref. [4].

2.2 Murmur Vector Composed of Principal Components

The property of the stenosis signal is investigated with point of view how it is reflected in the spectrum distribution. Figure 4 shows the power spectral densities of the sound pressures in Fig. 2. The sound pressures and their principal components were expressed by $x_{\ell,\sigma}^{(p)}(t)$ and $y_{\ell,\sigma}^{(p)}(t)$, respectively. These are transformed into the spectral densities $|X_{\ell,\sigma}^{(p)}(f)|^2$ and $|Y_{\ell,\sigma}^{(p)}(f)|^2$ respectively with the maximum entropy method (MEM). Here the degree of the autoregression polynomial is $N_{\text{MEM}} = 128$ and the number of frequencies at which the spectrum intensities are obtained is set to be $N_{\text{MEM}} + 1$. The panels in column (a) and (b) show how the spectrum distribution depends on the captured site and the principal component, respectively. The solid and dashed curves stand for the data being captured before and after the surgery PTA, respectively. In the spectrum distribution at site 2, the spectrum intensity before PTA becoms smaller after PTA in the high frequency region. This distribution at high frequencies corresponds the trembling behaviour of site 2 in time domain that is shown in Fig. 2 (a). The change of distribution is reflected in the 4th component as shown in the column in Fig. 4 (b). Furthermore, the peaks near 200 Hz disappear after PTA in panels of column (a) except the site 4. The frequency of this peak was termed as the break frequency, which characterizes the stenosis [4]. The
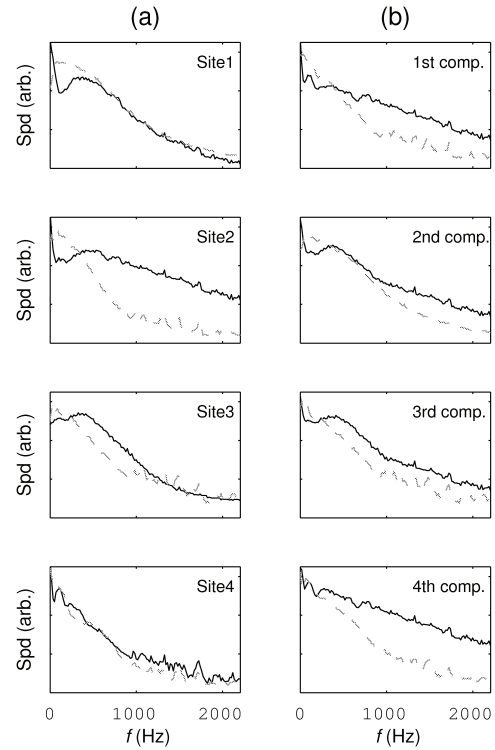

Fig. 4 Change of spectrum before (solid curve) and after (dashed curve) the surgery PTA. Variation due to (a) capture sites, $\xi_{\ell,\sigma}(f)$, and (b) pricipal components, $\eta_{\ell,\sigma}(f)$ ($\ell = 1, 2, 3, 4$, $\sigma = $ bfr/aft).

disappearance of the peaks is reflected in the change of the 3rd principal component as shown in the column (b). As mentioned above, the peculiar property of the captured murmurs is mainly reflected in the 3rd and 4th components of PCA.

The averages of the spectral densities by pulses are defined as follows:

$$\xi_{\ell,\sigma}(f) = \frac{1}{P} \sum_{p=1}^{P} \log_{10} |X_{\ell,\sigma}^{(p)}(f)|^2, \tag{4}$$

$$\eta_{\ell,\sigma}(f) = \frac{1}{P} \sum_{p=1}^{P} \log_{10} |Y_{\ell,\sigma}^{(p)}(f)|^2. \tag{5}$$

Furthermore, the spectrum vector $\mathbf{z}_{\ell,\sigma}$ is composed of the ℓ-th components $\eta_{\ell,\sigma}(f)$ as follows: $\mathbf{z}_{\ell,\sigma} = [\eta_{\ell,\sigma}(f_0)\ \eta_{\ell,\sigma}(f_1)\ \eta_{\ell,\sigma}(f_2)\ \ldots \eta_{\ell,\sigma}(f_{N_{\text{MEM}}})]^T$. For characterizing the stenosis feature included in the shunt murmur, we defined the new vector as $\mathbf{m}_\sigma = [\mathbf{z}_{3,\sigma}\ \mathbf{z}_{4,\sigma}]^T$, which is hereafter termed as *murmur vector*. Here the discretized frequency f_q is set to be $f_q = qF_s/2N_{\text{MEM}}$ ($q = 0, 1, 2, \ldots, N_{\text{MEM}}$) and the dimension of the vector is $2(N_{\text{MEM}} + 1)$ (= 258). As already mentioned, the sum of squares of the sound pressure in the time domain was normalized to be unity.

2.3 The Estimate of Stenosis Site

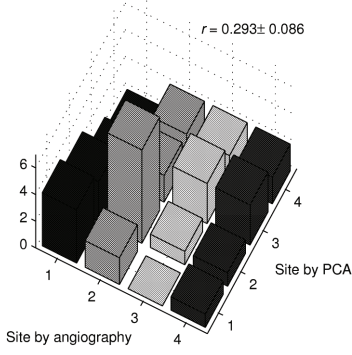In Fig. 2 (a), the dominant signal is the global oscillating

Fig. 5 Correlation between the stenosis sites confirmed by angiography and estimated by PCA.

Fig. 6 Hierarchical categorization of learning data by rs-SOM.

motion that is caused by the heartbeat. In contrast, in the wave form at site 3 ($\ell = 3$), the component involved in the heartbeat is not significant. Therefore, the wave form can be regarded to be under strong influence of stenosis at the site 2. Moreover, in the wave form shown in Fig. 2 (b), the form of 4th ($=L$-th) component is mostly similar to the spectrum at site 2. The L-th component has the minimum displacement from the hyperplane determining the correlation and reflects the most peculiar signal among the captured sites. From the reasons listed above, the peculiar feature at site 2 can be regarded to be caused by the stenosis.

If we defined the distance between the spectral densities, we can quantitatively discuss the above mentioned estimate about the stenosis site. One natural distance between the spectral densities of bare murmur captured from the forearm, $\xi_{\ell,\mathrm{bfr}}(f_q)$, and the L-th component derived by PCA, $\eta_{L,\mathrm{bfr}}(f_q)$, is the Euclidian distanc $\|\xi_{\ell,\mathrm{bft}} - \eta_{L,\mathrm{bft}}\|$, which is defined as follows:

$$\|\xi_{\ell,\mathrm{bft}} - \eta_{L,\mathrm{bft}}\| = \left\{ \sum_{q=0}^{N_{\mathrm{MEM}}} \left(\xi_{\ell,\mathrm{bfr}}(f_q) - \eta_{L,\mathrm{bfr}}(f_q) \right)^2 \right\}^{1/2}. \quad (6)$$

Then, the stenosis site can be estimated to be at ℓ-th site that gives the minimum of $\|\xi_{\ell,\mathrm{bfr}} - \eta_{L,\mathrm{bfr}}\|$. Figure 5 shows the three-dimensional histogram of the relation between the estimated site and the actual site confirmed by the angiography. The total number of data is 45 and the correlation coefficient r is $r = 0.293$ with the propability error 0.086. Although the correlation is not perfect, the significant estimate of the stenosis site is possible.

3. Stenosis Assessment

3.1 The Hierarchical Categorization by rs-SOM

The shunt murmur includes various information such as the heartbeat and the vessel situation. Among various shunt murmurs, typical data were empirically gathered and classified into five categories: N A, B, C and I [10]. Using the index α (= N, A, B, C, I) to indicate the category, the murmur vector can be expressed as $\mathbf{m}_{\sigma,\beta}^{(\mathrm{Emp},\alpha)}(\beta = 1, 2, \ldots, B_\alpha)$. Here, B_α is the element number of the category with index
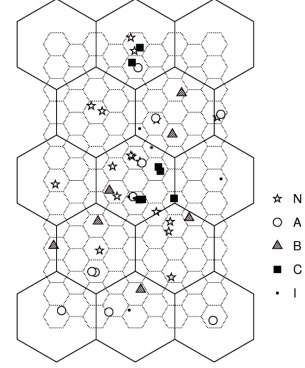
α. A set of the element numbers of these empirical categories was given as follows: $B_{\mathrm{N}} = 12$, $B_{\mathrm{A}} = 9$, $B_{\mathrm{B}} = 7$, $B_{\mathrm{C}} = 6$ and $B_{\mathrm{I}} = 6$. The empirical categories can be reproduced by the artificial categorization of SOM [10]. In this study, the interpolated model vectors are generated by using the hierarchical categorization realized by rs-SOM and applied to assessment the hemodialysis stenosis.

In Fig. 6, the characteristic map made by rs-SOM is shown, which was generated with the learning data composed of the above mentioned typical murmurs and newly included thirteen data. The lerning data are composed of murmur vectors before and after PTA as $\mathbf{M}_\beta = [\mathbf{m}_{\mathrm{aft},\beta} \ \mathbf{m}_{\mathrm{bfr},\beta}]^T$ ($\beta = 1,2, \ldots, N_{\mathrm{lrn}}$). The reason to introduce these composite vectors is to consider the vessel state with and without stenosis signal. The system parameters for rs-SOM [11] are as follows: The total number of learning data is $N_{\mathrm{lrn}} = 53$. The dimension of the composite model vector $\mathbf{M}_\beta$ for learning data is $4(N_{\mathrm{MEM}} + 1)(= 516)$. The type of distance between the data is Euclidian. The hexagon cell number of initial and the second generation $A^{(s)}$ ($s = 1, 2$) are $A^{(1)} = 13$ and $A^{(2)} = 113$. Update of the composite model vectors in the map was repeated at least five and less than two hundred until the rearrangement of the learning data did not occur.

In Fig. 6, the hexagons with black and gray lines correspond to the categories in the initial and the second generation, respectively. Each marker represents one of the learning data and its shape indicates the empirical category shown in the legend. The hexagon cell to which the marker was mapped is the category of the murmur vector. For example, the shunt murmurs symbolized by the circles and triangles were distinguishable by the auscultation by ear; those markers are separately mapped to the different hexagons of gray lines. On the contrary, the shunt murmurs symbolized by squares were difficult to be told what is the difference but those were empirically apparent to be caused by stenosis [10]. Therefore, several squares coexist with other maker at the same hexagon of gray lines. The categorisation by rs-SOM realizes the reasonable and minute classification without the assistance of experience.

Using the hierarchical categorization of the rs-SOM, the categories and their composite model vectors can be

generated by interpolating the differences of the learning data expressed by the composite vecoter $\mathbf{M}_\beta$. Each black hexagon at the initial generation can be regarded as the α-th category, which is composed of composite model vectors allocated to each of the gray hexagons being nested in the black hexagon. The composite model vectors which were allocated to gray hexagons can be expressed by dividing in two as follows: $[\mathbf{m}^{(SOM,\alpha)}_{aft,\beta} \ \mathbf{m}^{(SOM,\alpha)}_{bfr,\beta}]^T$ with the category index α for the black hexagon and the element index β (= 1, 2, ..., B_α) for the gray hexagons. Therefore, each component of the murmur vector, $\mathbf{m}^{(SOM,\alpha)}_{\sigma,\beta}$ (σ = bfr/aft), can be used as a model of shunt murmurs which change before and after PTA. The number of the category is $A^{(1)} = 13$ and the number of murmur vectors B_α belonging to the α-th category is any of {19, 12, 11, 7} which is determined by the location in the characteristic map of SOM.

Many gray hexagons include no learning data in Fig. 6. The composite model vectors representing these hexagons are generated by interpolating the difference of learning data belonging to neighbour cells. Even if any of singular data is included in the learning data, the singularity tends to be eased and a moderate model vector can be generated using the information from the neighbour cells. These feature can be realized by the hierarchical categorization of rs-SOM. In the next section, the stenosis assessment is defined using two types of model vectors, which are $\mathbf{m}^{(Emp,\alpha)}_{\sigma,\beta}$ belonging to the empirical category and $\mathbf{m}^{(SOM,\alpha)}_{\sigma,\beta}$ belonging to the SOM category.

3.2 Stenosis Level

For quantifying how the stenosis worsens, we shall define the stenosis level. For the first step, to quantify the difference between a murmur vector $\mathbf{m}$ and the model vectors belonging to the category α, the distance between these is introduced as follows:

$$d^{(\Gamma,\alpha)}_\sigma(\mathbf{m}) = \frac{1}{B_\alpha} \sum_{\beta=1}^{B_\alpha} \|\mathbf{m} - \mathbf{m}^{(\Gamma,\alpha)}_{\sigma,\beta}\|. \quad (7)$$

Here $\mathbf{m}^{(\Gamma,\alpha)}_{\sigma,\beta}$ are components of the composite model vectors of the category α (Γ = Emp/SOM, σ = bfr/aft, β = 1, 2, ..., B_α), and $\|\mathbf{m} - \mathbf{m}^{(\Gamma,\alpha)}_{\sigma,\beta}\|$ means Euclidian distance. Furthermore, the distance from the state with or without stenosis $c^{(Emp/SOM)}_\sigma(\mathbf{m})$ (σ = bfr/aft) can be measured as

$$c^{(Emp)}_\sigma(\mathbf{m}) = \min \left\{ d^{(Emp,\alpha)}_\sigma(\mathbf{m}) \,\Big|\, \alpha = N, A, B, C, I \right\} \quad (8)$$

under using the empirical category or

$$c^{(SOM)}_\sigma(\mathbf{m}) = \min \left\{ d^{(SOM,\alpha)}_\sigma(\mathbf{m}) \,\Big|\, \alpha = 1, 2, \ldots, A^{(1)} \right\} \quad (9)$$

under using the SOM category. Although the distance $c^{(\Gamma)}_{aft}(\mathbf{m})$ itself can be used to measure the progress of stenosis, the relative distance $S^{(\Gamma)}(\mathbf{m})$ is defined as follows:

$$S^{(\Gamma)}(\mathbf{m}) = \frac{c^{(\Gamma)}_{aft}(\mathbf{m})}{c^{(\Gamma)}_{aft}(\mathbf{m}) + c^{(\Gamma)}_{bfr}(\mathbf{m})}. \quad (10)$$

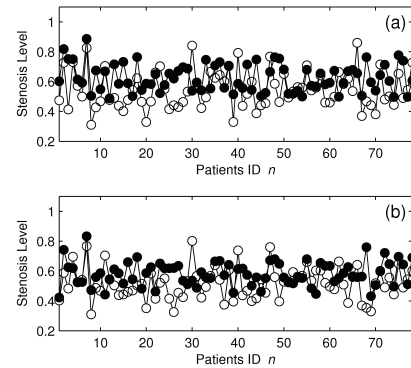**Fig. 7** Change of stenosis levels for each of patients before and after PTA being denoted by ● and ○, respectively. The stenosis levels are derived with (a) the SOM category, $S^{(SOM)}(\mathbf{m}_{\sigma,n})$, and (b) the empirical category, $S^{(Emp)}(\mathbf{m}_{\sigma,n})$, ($\sigma$ = bfr/aft, n = 1, 2, ..., 78).

The value of quantity $S^{(\Gamma)}(\mathbf{m})$ is normalized to be in the interval [0, 1]. Therefore, the misfit of distances between the categories can be adjusted. The relative distance $S^{(\Gamma)}(\mathbf{m})$ is termed as the *stenosis level* of the murmur vector $\mathbf{m}$ with the category Γ(= Emp/SOM).

3.3 Stenosis Assessment and ROC Diagram

In Fig. 7, the change of stenosis levels is shown with the data of 78 different from the learning data. The panels (a) and (b) differ in the categories; these are the emprical (Γ = Emp) or SOM (Γ = SOM). The horizontal and vertical axis are the patient ID n and the stenosis levels $S^{(\Gamma)}(\mathbf{m}_{\sigma,n})$, respectively. Here, $\mathbf{m}_{\sigma,n}$ is the murmur vector of each patient with the ID number n (= 1, 2, ..., 78) and the PTA index σ (= bfr/aft). The ● and ○ stand for the data before and after the surgery PTA, respectively. The levels of ○ tend to be smaller than those of ●. The span of change from ● to ○ is certainly wider in panel (a) than in pannel (b). This difference affects the efficiency of the stenosis assessment.

Using the threshold criterion, we can assess whether a patient has the stenosis. If the stenosis level $S^{(\Gamma)}(\mathbf{m}_{\sigma,n})$ exceeded a certain threshold S_{th}, the stenosis is suspected to exist. Two important rates under the assessment are the miss rate N_{miss} and the excess rate N_{exc}. The former one N_{miss} is the false-negative rate of patients satisfying $S^{(\Gamma)}(\mathbf{m}_{bfr,n}) < S_{th}$. The later one N_{exc} is the faulse-positive rate of patients satisfying $S^{(\Gamma)}(\mathbf{m}_{afr,n}) \geq S_{th}$. If the system is used to find patients who needs another accurate but harmful investigation such as angiography, no patient suspected to be positive must be missed. The efficiency of the assessment under this usage, can be evaluated by the excess rate N_{exc} when $N_{miss} = 0$. This value is expressed as N^*_{exc}.

In Fig. 8, the relation between the excess rate N_{exc} and miss rate N_{miss} are summarize in the receiver operating characteristic (ROC) diagram [15] when the empirical (Γ = Emp) and SOM (Γ = SOM) categoris are used to calculate the stenosis level. The critical value N^*_{exc} is the intercept of the
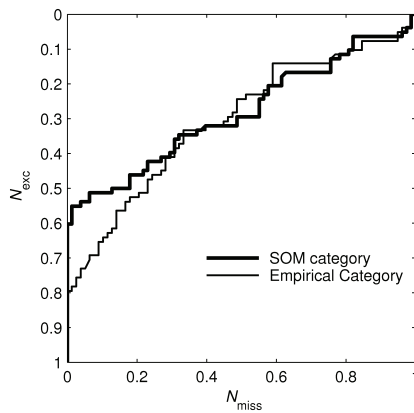
Fig. 8 ROC diagram of the stenosis assessment with the threshold criterion.

curves and the vertical axis. The value of N_{exc}^* was improved by an amount of 0.20 as the category is updated from empirical ($N_{\text{exc}}^* = 0.80$) to SOM ($N_{\text{exc}}^* = 0.60$). Considering the perfectness of finding stenosis, $N_{\text{miss}} = 0$, the correctness rate of the assessment reaches 0.7 ($= 1 - 0.5 N_{\text{miss}} - 0.5 N_{\text{exc}}^*$), which is sufficient in clinical fields. Further improvement can be realized by the update of the database and/or the data tracing of each individual patient.

4. Conclusion

Capturing the shunt murmurs from four sites in forearm and applying PCA to extract the stenosis signal, we have developed an estimate method for the first time to find where the stenosis is located. The significance of the estimate was evaluated by the correlation coefficient of 0.293, which was confirmed by angiography.

The excess positive rate N_{exc}^* of the stenosis assessment was improved by the amount of 0.20. This improvement was realized using the new definition of stenosis level and the hierarchical categorization of learning data realized by rs-SOM.

References

[1] P.J. Bosman, F.T.J. Boereboom, H.F.M. Smits, B.C. Eikelboom, H.A. Koomans, and P.J. Blankestijn, "Pressure or flow recordings for the surveillance of hemodialysis grafts," Kidney International, vol.52, no.4, pp.1084–1088, 1997.

[2] U. Ozyer, A. Harman, C. Aytekin, F. Boyvat, and F. Karakayali, "Application of the AMPLATZER vascular plug in endovascular occlusion of dialysis accesses," CardioVascular and Interventional Radiology, vol.32, no.5, pp.967–973, 2009.

[3] A. Asif, D. Merrill, P. Briones, D. Roth, and G.A. Beathard, "Hemodialysis vascular access percutaneous interventions by nephrologists," Seminars in Dialysis, vol.17, no.6, pp.528–534, 2004.

[4] P. Ask, B. Höek, D. Loyd, and H. Teriö, "Bio-acoustic signals from stenotic tube flow: state of the art and perspectives for future methodological development," Med. Biol. Eng. Comput., vol.33, no.5, pp.669–675, 1995.

[5] H.A. Mansy, S.J. Hoxie, N.H. Patel, and R.H. Sandler, "Computerized analysis of auscultatory sounds associated with vascular patency of haemodialysis access," Med. Biol. Eng. Comput., vol.43, no.1, pp.56–62, 2005.

[6] T. Sato, K. Tsuji, N. Kawashima, T. Agishi, and H. Toma, "Evaluation of blood access dysfunction based on a wavelet transform analysis of shunt murmurs," Journal of Artificial Organs, vol.9, no.2, pp.97–104, 2006.

[7] A. Murakami, K. Niizuma, Y. Motohashi, T. Sato, N. Kawashima, T. Shibuya, E. Takagi, T. Motohashi, T. Hoshino, T. Agishi, and K. Omi, "Noninvasive biofunctional diagnosis based on time-frequency analysis of various biosounds," IEICE Technical Report, US2009-25, 2009.

[8] H. Waki, Y. Suzuki, O. Sakata, M. Fukasawa, and H. Kato, "Auscultating diagnosis for hemodialysis shunt stenosis using a self-organizing map and hidden Markov model," IEEJ Transactions on Electronics, Information and Systems, vol.132, no.10, pp.1589–1594, 2012.

[9] M. Kiryu, H. Kato, Y. Suzuki, M. Fukasawa, and O. Sakata, "Classification of stenosis signals in shunt murmurs using nonsteady oscillation model," IEICE Technical Report, MBE2014-34, 2014.

[10] Y. Suzuki, M. Fukasawa, T. Mori, O. Sakata, A. Hattori, and T. Kato, "Elemental study on auscultating diagnosis support system of hemodialysis shunt stenosis by ANN," IEEJ Transactions on Electronics, Information and Systems, vol.130, no.3, pp.401–406, 2010.

[11] H. Kato, Y. Suzuki, M. Fukasawa, O. Sakata, and A. Hattori, "Proposal of categorization and stenosis screening of shunt sounds by recursive subdivision self-organizing map," IEICE Trans. Inf. & Syst. (Japanese Edition), vol.J95-D, no.1, pp.139–148, Jan. 2012.

[12] I.T. Jollife, Principal Component Analysis, second ed., Chap. 1 and Chap. 2, Springer, New York 2002.

[13] S. Suzuki, O. Sakata, M. Fukasawa, and H. Kato, "Elemental development of the shunt stenosis screening equipment using multichannel sensors," Proc. 12th Information Science Technology Forum, Tottori, Japan, pp.413–414, Sept. 2013.

[14] T. Kohonen, Self-Organizing Maps, third ed., Springer, New York, 2001.

[15] P. Egan, Signal Ddetection Theory and ROC Analysis, Academic Press, New York, 1975.